Developing a Laptop Power Adaptor for 12 V and 24 V Solar PV Source

L. Chilumba[1,2], A.T. Mushi[1], and B.M.M. Mwinyiwiwa[1]
[1] University of Dar es Salaam, Tanzania
[2] Vocational Education Authority of Tanzania, Tanzania

***Abstract*-- Rural and urban areas of developing countries such as Tanzania suffer from lack of reliable electricity supply. This situation limits the usage of portable electronic gadgets such as laptops, and mobile phones. This paper designs and simulates a laptop charger adapter using a DC-DC single ended primary inductor converter (SEPIC). This charging adapter accepts two voltage levels of varying sources of solar photovoltaic (PV) power. Its output is constant DC at 19.5 V and maximum 100 W power while input is either the variable 12 V or 24 V solar PV power source. The maximum power point (MPPT) algorithm is integrated with proportional integral (PI) controller to achieve the desired output. This design was validated numerically using the MATLAB/Simulink environment. Several results are presented showing the performance with the cases of varying solar irradiation from 800 W/m^2 to 1000 W/m^2 or vice versa. These simulation results indicate possibility of future work of the viability to fabricate the adaptor and test it in laboratory and in field.**

***Index Terms*—Renewable energy, Converter, Tanzania, Maximum power point tracking.**

I. Introduction

The world population is estimated to reach 8.5 billion by the year 2030 from the current 7.7 billion [1], and 61.7 million of these live in Tanzania as per the Tanzania National Census of 2022 [2]. This translates to high demand of electricity to power various human applications such as charging mobile phones, tablets and laptops. However, in Tanzania rural and urban areas, the electricity access is slightly over 78% [3], [4], and the reliability is not always guaranteed [5]–[7], while the electric utility company (Tanzania Electric Supply Company (TANESCO)) [8] tries its best to rectify this situation. This inaccessibility and unreliability causes the charging of laptops to be a problem, especially in the rural and urban areas when there is no electricity from the grid [9]. There are efforts to use microgrids to generate electricity using available renewable energy resources such as solar photovoltaic, hydro, wind and geothermal [10], [11], and if successful they can be used to supply these energy demands.

It is therefore important to use solar photovoltaics (PV) to generate electricity for powering and charging laptop chargers/adaptors [12]. The harnessing of solar PV power has gained a lot of interests lately, for example these works [13]–[15], and due to high laboratory efficiencies of solar cells [16] their use for solar PV power generation is projected to increase. However, due to the intermittency nature of these solar PV power, a controlled DC-DC converter is needed to harness this power in the maximum power points (MPP). One such converter is single ended primary inductor converter (SEPIC). This converter will work with an algorithm to harness maximum power, that is, maximum power point tracking (MPPT) which is coupled to a proportional integral (PI) controller.

II. Solar PV Charger Architecture

The solar PV charger architecture comprises of the following – solar PV array, SEPIC converter (DC/DC), controller and measurement sensors. This configuration is shown in Fig. 1. The solar PV array is receiving insolation $G(t)$, at temperature $T(t)$. The solar PV generates current I_{PV}, at terminal voltage V_{PV}. The converter gives output voltage V_O, while the measuring system collects the output voltage and current for control purposes.

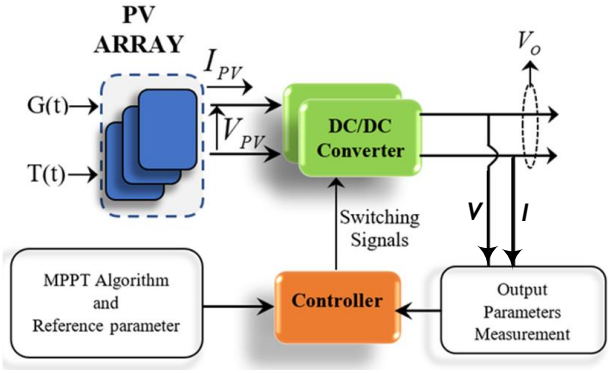

Fig. 1. Solar PV charger architecture

A. Solar PV Array

The solar PV array shown in Fig. 1 is made up of several solar panels. These are made of solar cells in arrangements that give the required voltages and currents. A solar cell can be modeled as a light dependent current source in parallel with a diode and shunt resistor. This combination is in series to a resistor through which the cell current and terminal voltage can be collected [17], [18]. For the interested readers, they can find other solar PV array models in [19], [20].

B. SEPIC Converter

The SEPIC converter is configured as shown in Fig. 2, where source is V_{PV}, inductors 1 and 2 are L_1 and L_2, capacitors 1 and 2 are C_1 and C_2, the load being R and an output voltage V_O. This converter is controlled by MPPT and PI control algorithms to enable constant output charging voltage [12].

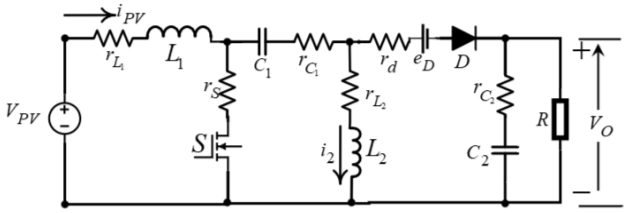

Fig. 2. SEPIC DC-DC converter

All the converter's parasitics are considered as shown in Fig. 2. The converter's state space (after small signal averaging such as [21] is obtained by (1) – (2), where $\hat{x}(t)=\left[\hat{i}_{PV}(t)\,\hat{i}_{L2}(t)\,\hat{v}_{C1}(t)\,\hat{v}_{C2}(t)\right]^T$. The matrices $[A]$, $[B]$ and $[C]$ are defined by (3) – (18) for which detailed procedure is found in [12]. One must note that, the upper letter case variables (V_{C1}, V_{C2}, I_{L2}, I_{PV}, and D) are the steady states.

$$\frac{d}{dt}\hat{x}(t)=A\hat{x}(t)+B\hat{v}_{PV}(t)+C\hat{d}(t) \tag{1}$$

$$\hat{v}_0(t)=\left(\frac{Rr_{C2}}{R+r_{C2}}\right)\left(\hat{i}_{PV}(t)+\hat{i}_{L2}(t)\right)+\left(\frac{R}{R+r_{C2}}\right)\hat{v}_{C2}(t) \tag{2}$$

$$[A]=\begin{bmatrix}A_{11}&A_{12}&A_{13}&A_{14}\\A_{21}&A_{22}&A_{23}&A_{24}\\A_{31}&A_{32}&A_{33}&A_{34}\\A_{41}&A_{42}&A_{43}&A_{44}\end{bmatrix} \tag{3}$$

$$[B]=\begin{bmatrix}\frac{1}{L_1}&0&0&0\end{bmatrix}^T \tag{4}$$

$$[C]=\begin{bmatrix}-C_{11}\\\frac{V_{C1}-I_{L2}r_{C1}+a_2I_{PV}+e_D+a_3V_{C2}}{L_2}\\-\left(\frac{I_{PV}+I_{L2}}{C_1}\right)\\-\left(\frac{I_{PV}+I_{L2}}{C_2}\right)\end{bmatrix} \tag{5}$$

$$A_{11}=-\frac{a_1D-a_1-r_{C1}-Dr_S}{L_1} \tag{6}$$

$$A_{12}=\frac{a_1D-a_2-Dr_S}{L_1} \tag{7}$$

$$A_{13}=\frac{1-D}{L_1},\quad A_{14}=\frac{a_3-D}{L_1} \tag{8}$$

$$A_{21}=\frac{a_2D-a_2-r_S}{L_2} \tag{9}$$

$$A_{22}=-\frac{r_{L2}+Dr_{C1}+r_S}{L_2} \tag{10}$$

$$A_{23}=-\frac{D}{L_2},\quad A_{24}=-\frac{a_3(1-D)}{L_2} \tag{11}$$

$$A_{31}=\frac{1-D}{C_1},\quad A_{32}=-\frac{D}{C_1} \tag{12}$$

$$A_{33}=A_{34}=0 \tag{13}$$

$$A_{41}=A_{42}=\frac{a_3(1-D)}{C_2},\quad A_{43}=0 \tag{14}$$

$$A_{44}=\frac{1}{C_2(R+r_{C2})} \tag{15}$$

$$a_1=r_{C1}+r_d+\frac{Rr_{C2}}{R+r_{C2}} \tag{16}$$

$$a_2=r_d+\frac{Rr_{C2}}{R+r_{C2}},\quad a_3=\frac{R}{R+r_{C2}} \tag{17}$$

$$C_{11}=\frac{a_1I_{PV}+a_2I_{L2}+V_{C1}+e_D+a_3V_{C2}-r_S(I_{PV}+I_{L2})}{L_1} \tag{18}$$

C. SEPIC Converter Components Sizing

The SEPIC converter has four main active components which are designed based on steady state conditions. The average steady state solar PV voltage V_{PV} obtained for a steady state duty ratio D, supplying steady state power, voltage and current (P_O, V_O, and I_O) is summarized by (19). The allowed ripple on voltages and currents on the components is summarized by (20). From (19) – (22), the inductors and capacitors are sized according to (23) – (26), and values are listed in Table 1.

$$V_O=\frac{D}{1-D}V_{PV},\quad V_{C1}=V_{PV},\quad V_{C2}=V_O \tag{19}$$

$$I_{L1}=\frac{D}{1-D}I_O,\quad I_{L2}=I_O \tag{20}$$

$$\Delta i_{L1}=\frac{V_{PV}DT_s}{L_1},\quad \Delta i_{L2}=\frac{V_O(1-D)T_s}{L_2} \tag{21}$$

$$\Delta v_{C1}=\frac{I_ODT_s}{C_1},\quad \Delta v_{C2}=\frac{I_ODT_s}{C_2} \tag{22}$$

$$L_1\geq\frac{V_{PV\max}^2V_OT_s}{\frac{\Delta i_{L1}}{I_{PV}}(V_{PV\max}+V_O)P_O} \tag{23}$$

$$L_2\geq\frac{V_O^2V_{PV\max}T_s}{\frac{\Delta i_{L2}}{I_O}(V_{PV\max}+V_O)P_O} \tag{24}$$

$$C_1\geq\frac{P_OT_s}{\frac{\Delta v_{C1}}{V_{PV\min}}(V_{PV\max}+V_O)V_{PV\min}} \tag{25}$$

$$C_2 \geq \frac{P_O T_s}{\frac{\Delta v_{C2}}{V_O}\left(V_{PV\max} + V_O\right)V_O} \tag{26}$$

TABLE I
SEPIC CONVERTER DESIGN SPECIFICATIONS

Parameter	Value range	Component	Size
V_{PV}	12 V to 24 V	L_1	850 µH
$V_{PV\min}$, $V_{PV\max}$	9.8 V, 27 V		
V_O , P_O	19.5 V, 100 W	L_2	600 µH
$\frac{\Delta i_{L1}}{I_{PV}}$, $\frac{\Delta i_{L2}}{I_O}$	0.05, 0.05	C_1	45 µF
$\frac{\Delta v_{C1}}{V_{PV\min}}$, $\frac{\Delta v_{C2}}{V_O}$	0.08, 0.08	C_2	100 µF
f_s , T_s	50 kHz, 0.02 ms		
r_d , r_s , e_D	0.1 Ω, 0.18 Ω, 1.67 V		
K_{P2} , K_{I2}	0.0001, 0.01		
K_{P1} , K_{I1}	0.01, 10		

D. The Feedback Controller

The SEPIC converter for the solar PV application is augmented with a proportional integral controller (PI), which works in conjunction with an MPPT algorithm as shown in Fig. 3. The algorithm for the MPPT can be found in [11], [22], shown in Fig. 4, and that of the PI is easily accessed such as from [21]. The MPPT considers the voltage at time instant k, as $V(k)$, current as $I(k)$ power as $P(k)$, differential power variation as $dP(k)$, duty cycle as $D(k)$ and differential duty cycle variation as $dD(k)$. The PI processes duty cycles denoted by d_1, d_2 and D_m.

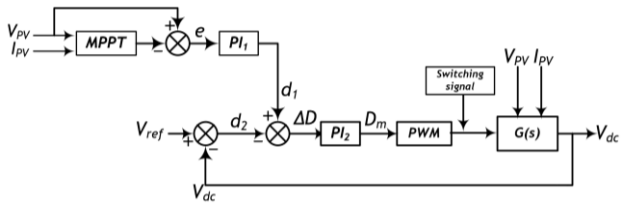

Fig. 3. The PI controller augmented with MPPT algorithm for the SEPIC converter.

The authors did not implement faster response time control algorithm such as the deadbeat controller [23]–[26], to avoid the longer computation times, because for this application it was deemed unnecessary.

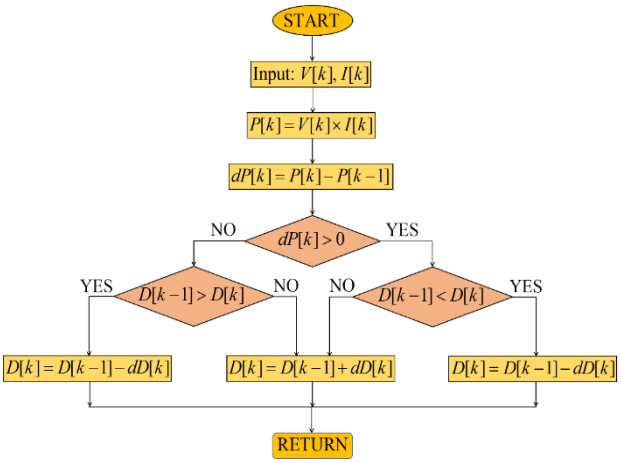

Fig. 4. The MPPT algorithm.

III. SIMULATION

The designed SEPIC converter, the solar PV, and the designed MPPT coupled to PI controllers were built and simulated in MATLAB/Simulink environment as shown in Fig. 5. During simulations, two scenarios were considered: insolation decreasing and increasing for the case of 12 V and 24 V sources.

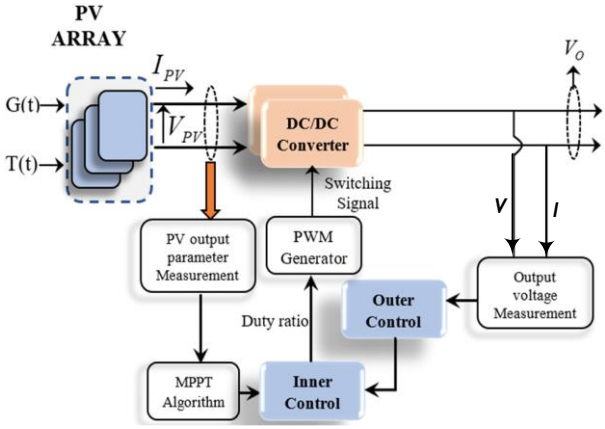

Fig. 5. The SEPIC converter with its control algorithms as implemented for simulations.

IV. RESULTS AND DISCUSSIONS

The two simulation scenarios' results are explained in this section.

A. The Case of 12 V Solar PV Source

The solar insolation decreasing from 1000 W/m^2 to 800 W/m^2 is depicted in Fig. 6, and Fig. 7 shows slight decrease of V_{PV} while the V_O tracks the reference with constant power output shown in Fig. 8 indicating a possibility to charge a laptop at decreased insolation.

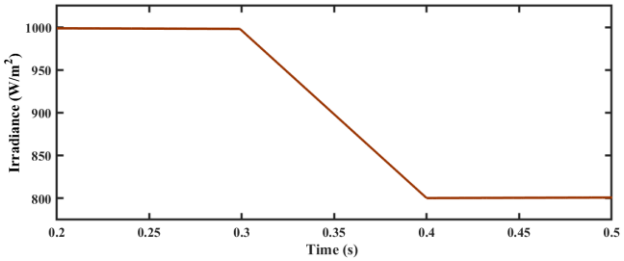

Fig. 6. The graph of decreasing solar insolation.

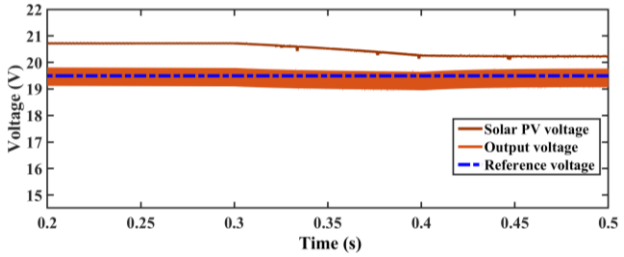

Fig. 7. The graphs of voltage decrease of V_{PV}, and V_O tracking the reference.

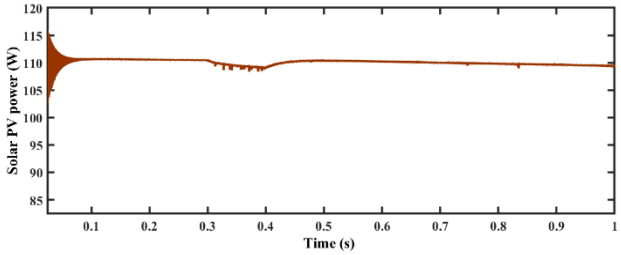

Fig. 8. Constant power output when insolation decrease.

The solar insolation increasing from 800 W/m^2 to 1000 W/m^2 is shown in Fig. 9. For this case, there is increase of V_{PV} while the V_O tracked the reference as shown in Fig. 10. These were accompanied by constant power output as shown in Fig. 11, indicating a possibility to charge a laptop at increased insolation.

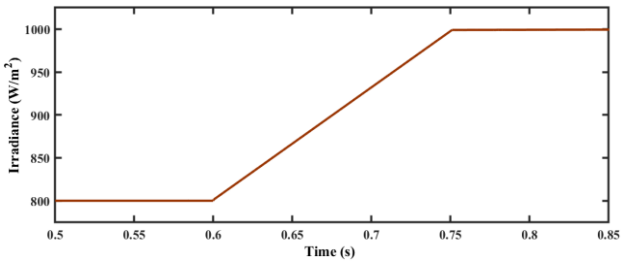

Fig. 9. The graph of increasing solar insolation.

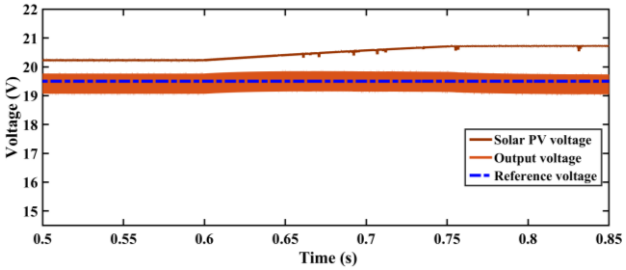

Fig. 10. The graphs of voltage increase of V_{PV}, and V_O tracking the reference.

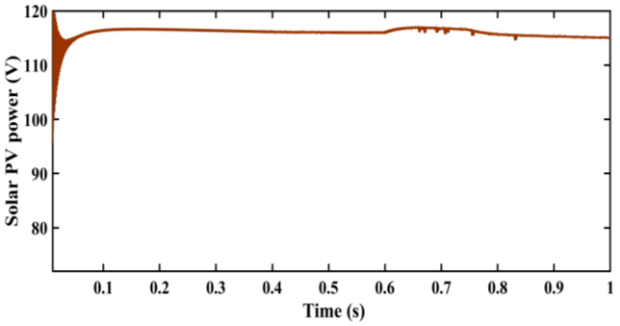

Fig. 11. The constant power output when insolation increased.

B. The Case of 24 V Solar PV Source

The solar insolation decreasing rapidly from 1000 W/m^2 to 800 W/m^2 is depicted in Fig. 12, and Fig. 13 shows the dipping of V_{PV} while the V_O tracks the reference indicating a possibility to charge the laptop even during sharp decrease of insolation at 24 V. This situation mimics a sudden cloud cover and the adaptor required to charge the laptop as shown in Fig. 13.

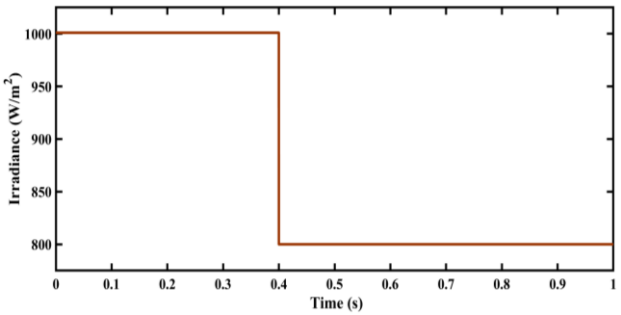

Fig. 12. The graph of rapid decrease of solar insolation representing a case of sudden cloudy cover.

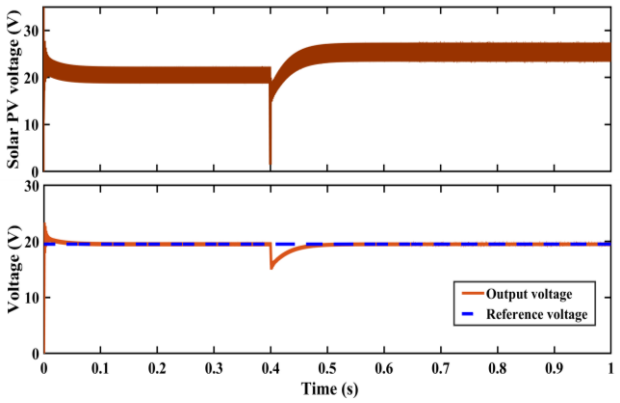

Fig. 13. The graphs of voltage rapid decrease of V_{PV} at the moment the insolation drops, and V_O dipping, and then tracking the reference.

The solar insolation increasing from 800 W/m^2 to 1000 W/m^2 is shown in Fig. 14. The V_{PV} and V_O are shown in Fig. 15. These indicate a possibility to charge a laptop at increased insolation.

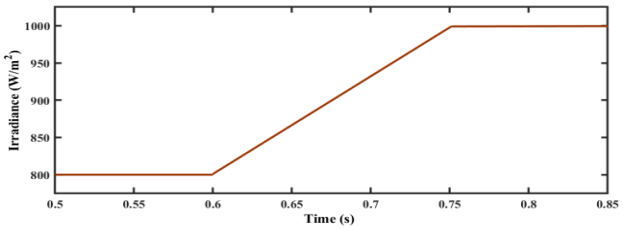

Fig. 14. The graphs of increasing solar insolation.

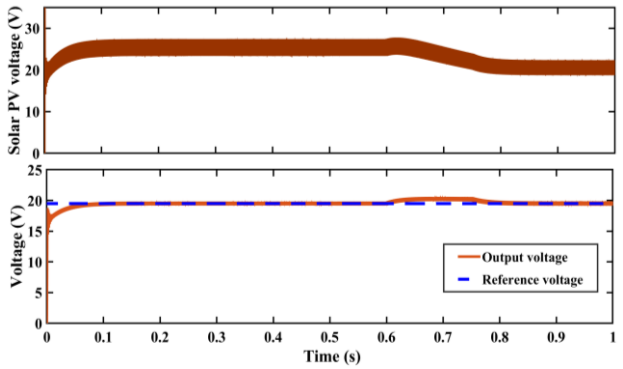

Fig. 15. The graphs of voltage V_{PV}, and V_O tracking the reference during the insolation increase.

V. Conclusions

This paper has designed a SEPIC converter to be used for laptop charger. The components were designed considering all the components' parasitics. The converter was controlled using PI controller and MPPT algorithms such that the output voltage was maintained constant for both increasing and decreasing solar insolation. This converter can work with either 12 V or 24 V input voltage from the solar PV and charge a laptop. The simulation results show that the converter at 12 V and at 24 V, can supply a constant DC load of up to 100 W regardless of slight insolation variations. This is a charger that can be useful for rural areas of Tanzania with no grid connection. Future work will involve fabricating of a prototype for experimental tests and implementing a faster control algorithm such as deadbeat controller for the SEPIC converter. This will be done in addition to field testing of the laptop charger and performing economic analysis to establish its feasibility for rural areas of Tanzania.

Acknowledgment

The authors are grateful to the University of Dar es Salaam (the College of Engineering and Technology), and the Vocational Education Authority of Tanzania for facilitating the research, and funding the paper presentation at ICPE 2023 ECCE-Asia.

References

[1] IEA, IRENA, UNSD, World Bank, and WHO, "TRACKING SDG7: The Energy Progress Report," Washington DC. , 2021. [Online]. Available: www.worldbank.org

[2] Wizara ya Fedha na Mipango, Ofisi ya Taifa ya Takwimu – Tanzania na Ofisi ya Rais – Fedha na Mipango, Ofisi ya Mtakwimu Mkuu wa Serikali Zanzibar, "Sensa ya Watu na Makazi ya Mwaka 2022: Matokeo ya Mwanzo," Dodoma, Oct. 2022. Accessed: Mar. 14, 2023. [Online]. Available: https://www.nbs.go.tz/nbs/takwimu/Census2022/matokeomwanzooktoba2022.pdf

[3] E. T. Marcel, J. Mutale, and A. T. Mushi, "Optimal Design of Hybrid Renewable Energy for Tanzania Rural Communities," *Tanzania Journal of Science*, vol. 47, no. 5, pp. 1716–1727, Dec. 2021, doi: 10.4314/tjs.v47i5.19.

[4] E. Nyanda, A. Mushi, and J. Justo, "Viability Analysis of Ubungo II Gas Power Plant Efficiency Improvement Using Co-generation System," *Tanzania Journal of Engineering and Technology*, vol. 41, no. 2, pp. 158–170, Aug. 2022, doi: 10.52339/tjet.v41i2.789.

[5] K. Makoye, "Drought cripples Tanzania's hydropower," 2022. [Online]. Available: https://www.aa.com.tr/en/africa/drought-cripples-tanzania-s-hydropower/2679268

[6] A. Mamun *et al.*, "Grid Electricity Expansion in Tanzania: Findings from a Rigorous Impact Evaluation INTERNATIONAL MCC energy sector project."

[7] Millennium Challenge Corporation, "Expanding Electricity Distribution in Tanzania," Mar. 2017.

[8] TANESCO, "TANESCO - Generation," 2022. https://tanesco.co.tz/index.php/about-us/functions/generation (accessed Jul. 28, 2022).

[9] L. J. Fungo, A. T. Mushi, and C. J. Msigwa, "Grid Connected PV-Wind Energy System for Luxmanda Village in Tanzania," in *The Third Annual Conference on Research and Inclusive Development*, Dodoma: University of Dar es Salaam, Nov. 2021.

[10] M. N. Minja and A. T. Mushi, "Design of International Airport Hybrid Renewable Energy System," *Tanzania Journal of Engineering and Technology*, vol. 42, no. 1, pp. 46–57, Feb. 2023, doi: 10.52339/tjet.v42i1.887.

[11] M. I. Juma, B. M. M. Mwinyiwiwa, C. J. Msigwa, and A. T. Mushi, "Design of a hybrid energy system with energy storage for standalone DC microgrid application," *Energies (Basel)*, vol. 14, no. 18, Sep. 2021, doi: 10.3390/en14185994.

[12] L. Chilumba, "Development of a Laptop Power Adaptor for 12 V and 24 V Solar Photovoltaic Sources," Masters, University of Dar es Salaam, Dar es Salaam, 2022.

[13] A. Aktaş and Y. Kirçiçek, "Solar Hybrid Systems and Energy Storage Systems," in *Solar Hybrid Systems*, Elsevier, 2021, pp. 87–125. doi: 10.1016/b978-0-323-88499-0.00005-7.

[14] A. Aly, M. Moner-Girona, S. Szabó, A. B. Pedersen, and S. S. Jensen, "Barriers to Large-scale Solar Power in Tanzania," *Energy for*

Sustainable Development, vol. 48, pp. 43–58, Feb. 2019, doi: 10.1016/j.esd.2018.10.009.

[15] A. Abd-Elfattah Darwish, R. S. Abdelmohsen, M. Ahmed, and M. Megeed, "Solar cells: Types, Modules, and Applications-A Review," *Tanzania Journal of Science*, vol. 48, no. 1, pp. 124–133, 2022, doi: 10.4314/tjs.v48i1.11.

[16] ISE and PSE, "Photovoltaics Report," Freiburg, Sep. 2022. Accessed: Nov. 11, 2022. [Online]. Available: https://www.ise.fraunhofer.de/content/dam/ise/de/documents/publications/studies/Photovoltaics-Report.pdf

[17] J. J. Justo and A. T. Mushi, "Performance Analysis of Renewable Energy Resources in Rural Areas: A Case Study of Solar Energy," *Tanzania Journal of Engineering and Technology (Tanz. J. Engrg. Technol.)*, vol. 39, no. 1, pp. 1–12, Jun. 2020, doi: https://doi.org/10.52339/tjet.v39i1.514.

[18] H.-L. Tsai, C.-S. Tu, and Y.-J. Su, "Development of Generalized Photovoltaic Model Using MATLAB/SIMULINK," in *Proceedings of the World Congress on Engineering and Computer Science*, IAENG International Association of Engineers, 2008.

[19] R. Khamharnphol *et al.*, "Microgrid Hybrid Solar/Wind/Diesel and Battery Energy Storage Power Generation System: Application to Koh Samui, Southern Thailand," *International Journal of Renewable Energy Development*, vol. 12, no. 2, pp. 216–226, Mar. 2023, doi: 10.14710/ijred.2023.47761.

[20] Energy Systems Integration Group, "Defining and Deploying Advanced, Grid-Forming Controls for Solar, Wind, and Battery Resources," 2022. Accessed: Jun. 13, 2023. [Online]. Available: https://www.esig.energy/wp-content/uploads/2022/03/ESIG-GFM-deployment-fact-sheet-2022.pdf

[21] A. Mushi, T. Nozaki, and A. Kawamura, "Proposal for faster disturbance rejection of boost DC-DC converter based on simplified current minor loop," in *2015 IEEE 2nd International Future Energy Electronics Conference, IFEEC 2015*, 2015. doi: 10.1109/IFEEC.2015.7361382.

[22] M. Juma, B. M. M. Mwinyiwiwa, C. J. Msigwa, and A. T. Mushi, "Proposal Design of a Hybrid Solar PV-Wind-Battery Energy Storage for Standalone DC Microgrid Application," 2021, doi: 10.20944/preprints202108.0264.v1.

[23] A. Mushi, S. Nagai, H. Obara, and A. Kawamura, "Fast and robust nonlinear deadbeat current control for boost converter," *IEEJ Journal of Industry Applications*, vol. 6, no. 5, 2017, doi: 10.1541/ieejjia.6.311.

[24] A. Mushi, S. Nagai, H. Obara, and A. Kawamura, "Design for nonlinear current reference deadbeat control for boost converter," in *2017 IEEE 3rd International Future Energy Electronics Conference and ECCE Asia, IFEEC - ECCE Asia 2017*, 2017. doi: 10.1109/IFEEC.2017.7992118.

[25] A. Khillo, S. S. Patnaik, and S. Naresh, "Performance Analysis of 6-Pulse HVDC-VSC using Deadbeat Controller in d-q Reference Frame under AC Fault Conditions," in *2020 IEEE 17th India Council International Conference (INDICON)*, IEEE, Dec. 2020, pp. 1–6. doi: 10.1109/INDICON49873.2020.9342337.

[26] Y. Kosode, H. Obara, A. Kawamura, Y. Hosoyamada, T. Suenaga, and I. Yuzurihara, "High Performance Transient Response of High/Low Pulse Voltage using Two-Phase Interleaved DC-DC Buck Converter under Half Sampling Time Deadbeat Control," *IEEJ Journal of Industry Applications*, vol. 9, no. 4, pp. 444–452, Jul. 2020, doi: 10.1541/ieejjia.9.444.